For a round tube (at n = 8)$U_{av}/U_0 = 0.837$, while $Q_B = \rho_B U_{av} \pi r_a^2$, we have

$$\rho_{s0} = 1{,}18K\rho_B(1 + 2A). \quad (7)$$

Finally from Eqs. (1) with allowance for (4) and (7) we obtain the distribution of the discrete-phase velocity and density at the exit from the tube.

As we see, the distribution of the discrete-phase parameters at the exit from the tube when a two-phase mixture flows through it depends on the carrier-phase parameters, the properties of the discrete pahse, and the geometrical characteristics of the channel. The data obtained can be used as limiting data in calculations of diverse technical equipment, both under study and under design.

NOTATION

U_0, carrier-phase velocity on the axis; U, carrier-phase velocity; U_{av}, average carrier-phase velocity; U_{s0}, discrete-phase velocity on the axis; U_s, discrete-phase velocity; d_s, average size of the solid-phase particles; γ_p, specific weight of the material of the particles; ρ_s, discrete-phase density in the stream (mass of particles per unit volume of stream); ρ_{s0}, discrete-phase density on the axis of the stream; ρ_B, carrier-phase density; Q_T, discrete-phase flow per second; Q_B, carrier-phase flow per second; $K = Q_T/Q_B$, solid-phase concentration in the stream; X, distance from the entry of the discrete phase into the tube to the exit cross section of the tube; D, diameter of the accelerating device; r_a, radius of the exit cross section of the nozzle; and g, gravitational acceleration.

LITERATURE CITED

1. B. A. Balanin and E. P. Trakhov, Flow of Viscous and Nonviscous Gases, Two-Phase Liquids [in Russian], Leningrad (1981).
2. N. N. Yanenko, R. I. Soloukhin, A. N. Payrin, and V. M. Fomin, Supersonic Two-Phase Flows Under the Conditions of Velocity Disequilibrium of Particles [in Russian], Novosibirsk (1980).
3. B. A. Balanin, S. A. Meladze, V. A. Chirukhin, and M. N. Chaika, Vestn. Leningr. Gos. Univ., No. 9, 32 (1986).
4. V. V. Zlobin, Inzh.-Fiz. Zh., 33, No. 4, 612.

PROPAGATION OF COMPRESSION WAVES IN A LONG VERTICAL CHANNEL CONTAINING A GASIFIED PACKET

S. D. Tseitlin

UDC 532.529.5:532.135

A solution is obtained for the problem of the pipe flow of a compressible non-Newtonian fluid involving the passage of a pressure pulse in annular and circular channels containing a homogeneous gas–liquid packet.

The study of processes connected with the transmission of compression waves in long channels filled with a non-Newtonian fluid – including gas-liquid packets – is of great interest. The need to solve such problems arises primarily when examining the subject of the prospecting and exploitation of oil and gas deposits. Fields that are being worked nearly always contain plugging and drilling fluids. These fluids, together with oil, have non-Newtonian properties and may contain gas–liquid occlusions of natural gas or air. The solutions obtained for these problems can also be used in the study of the dynamic processes occurring during the transfer of information along a hydraulic channel, during the pipe flow of fluids, in power engineering, etc.

In the course of solving the problems discussed above, it is also possible to study the way in which the transmission of dynamic disturbances in long channels is affected by the nonlinear viscosity and density of the fluid, the shape and dimensions of the cross section of the channel, and the presence of gas occlusions with different dimensions and

Central Geophysical Expedition, Moscow.

Translated from Inzhenerno-Fizicheskii Zhurnal, Vol. 8, No. 1, pp. 20-27, January, 1990. Original article submitted July 5, 1988.

0022-0841/90/5801-0014$12.50

gas contents. As has been shown by both theoretical and experimental studies (such as [1-3]) involving modeling of the transmission of dynamic disturbances in a channel, if an investigation is limited to disturbances of relatively low frequency (less than 10 Hz), it is possible to use a quasisteady approximation [2] of the system of equations which describes pipe flow with allowance for the effect of viscous friction:

$$\frac{\partial P}{\partial t} = -\frac{\rho c^2}{f}\frac{\partial q}{\partial z}, \quad \frac{\rho}{f}\frac{\partial q}{\partial t} = -\frac{\partial P}{\partial z} - \frac{\tau}{\delta}. \tag{1}$$

As an illustration of the solution of Eqs. (1), we will examine a problem involving determination of the presence of a gasified packet in the annular space of a gas test well at different times during the transmission of a pressure pulse generated at the well bottom by a special device. The pulse travels through a central circular pipe and the annular channel formed by this pipe and the wall of the well [4]. A difference arises in the time of passage of the pulse through channels of the same length due to its slowing in the case of the movement of a gasified column of liquid. The shape of the pulse is also distorted by viscous friction and the presence of boundaries where it is partially reflected. The problem just described arises in the study of the transmission of well-bottom data along a hydraulic channel.

We will examine a vertical channel of length L consisting of a central circular pipe with an inside diameter D and outside diameter D_2 (Fig. 1b). A liquid with the denstiy ρ and a rheology approximated by an exponential model wtih constant values of K and N ($\tau = K\dot{\gamma}^N$) flows down through the pipe at the rate q_0. The liquid is raised to the surface through the annular channel formed by the outside wall of the central pipe and another pipe of diameter D_1 positioned coaxially with respect to the first pipe. Part of the annular channel is filled by a gasified packet of length H_{gp} with a gas content α. Meanwhile, the lower boundary is located the distance X from the bottom. Since the processes connected with the propagation of dynamic perturbations in the channel occur incomparably more rapidly than the processes connected with the transport of the liquid and gas, we will consider the position of the gasified packet to be fixed and the gas-liquid mixture to be homogeneous. Then the speed of sound and density in the homogeneous gas-liquid mixture are determined in accordance with [5]:

$$c^2 = \left\{(\alpha\rho_g + (1-\alpha)\rho_\ell)\left(\frac{\alpha}{\rho_g c_g^2} + \frac{1-\alpha}{\rho_\ell c_\ell^2}\right)\right\}^{-1}, \tag{2}$$

$$\rho = \alpha\rho_g + (1-\alpha)\rho_\ell, \ \rho_g = \rho_{g0} P/P_{atm}.$$

With a gas content $\alpha = 0$ (absence of gas), $c = c_\ell$. With a gas content $\alpha = 1$ (absence of a liquid phase), $c = c_g$. It should be noted that the speed of sound in the gas–liquid mixture may be less than c_g and c_ℓ within a wide range of gas contents. Located at the bottom of the well ($z = 0$) is a special device which generates individual (or series of) pressure pulses through a time change in the cross section of the pipe along a certain part of its length. Here, a change may be realized in either the amplitude of the signal (ΔP_p^0), its duration (τ_{p1}, τ_{p2}), or its shape (k_1, k_2) in accordance with the following expression:

$$\Delta P_p(t) = \begin{cases} \Delta P_p^0 (t/\tau_{p1})^{k_1} & \text{at } 0 < t < \tau_{p1}, \\ \Delta P_p^0 \left(1 - \left(\dfrac{t-\tau_{p1}}{\tau_{p2}-\tau_{p1}}\right)^{k_2}\right) & \text{at } \tau_{p1} < t < \tau_{p2}, \\ 0 & \text{at } \tau > \tau_{p2}, \end{cases} \tag{3}$$

where $0 < \{k_1, k_2\} < 10$.

The shear stress on the wall during laminar flow of a fluid whose rheology is approximated by an exponential model is as follows: $\tau = K(\dot{\gamma}_1)^N = A_1\delta_1 q^N$, in the circular pipe; $\tau = K(\dot{\gamma}_2)^N = A_2\delta_2 q^N$, in the annular pipe. Here, $\dot{\gamma}_1$ and δ_1 are the shear velocity and the hydraulic radius of the annular space of the well. Thus, system (1) takes the following form for the problem being solved:

$$\frac{\partial P}{\partial t} = -\frac{\rho c^2}{f_i}\frac{\partial q}{\partial z}, \quad \frac{\partial q}{\partial t} = -\frac{f_i}{\rho}\left(\frac{\partial P}{\partial z} + A_i q^N\right), \ i = 1, 2, \tag{4}$$

where, in accordance with [4]:

$$A_1 = \frac{4K}{D}\left[\frac{8}{\pi D}\frac{3N+1}{N}\right]^N;$$
$$A_2 = \frac{4K}{D_1 - D_2}\left[\frac{16(2N+1)}{N\pi(D_1+D_2)(D_1-D_2)^2}\right]^N; \quad (5)$$

f_i being the cross-sectional area of the pipe.

The values of density ρ and the speed of sound c change along the channel in relation to the position, size, and gas content of the gas–liquid packet in accordance with Eqs. (2). The boundary condition at the inlet of the central pipe corresponds to a constant flow rate, i.e., $q(t, L) = q_0$. The boundary condition at the outlet of the annular pipe has the form: $P(t, L) = P_{atm} \simeq 10^5$ Pa. As the initial distributions of pressure and flow rate in the pipe, we took their distributions corresponding to steady flow with the rate q_0.

System of differential equations (4), describing the propagation of dynamic perturbations in pipes, is a hyperbolic system. One of the most natural methods of solving it is therefore the method of characteristics [2].

An analysis of Eqs. (4) indicates the existence of two families of characteristic curves with the slope $\gamma = dz/dt = \pm c$ in the plane (z, t). Thus, these curves have the form of straight lines with a slope corresponding to $\pm c_\ell$ in that part of the channel containing the nongasified liquid. Meanwhile, the slope of the characteristic curves is determined by Eq. (2) in the part of the channel where the gas–liquid packet is located. Two characteristic curves with different slopes emanate from the points corresponding to the boundaries of the liquid and gas–liquid packet (points 3"', 1"', 2"' in Fig. 1a). Since we chose a constant time step (T = h/c), this makes it necessary to establish different grid steps with respect to $z(h_j)$ in relation to the location of the grid node (j). Considering that the following relation is valid along the characteristic curve

$$\frac{d}{dt} = \frac{\partial}{\partial t} + \frac{\partial}{\partial z}\frac{dz}{dt},$$

and replacing the partial derivatives with respect to t in Eq. (4) by comlete differentials, we can obtain relations for the characteristic curves (the subscript i can be omitted):

$$\frac{f}{\rho}dP + cdq + \frac{cA}{\rho}q^N dt = 0, \quad dP - \frac{\rho c}{f}dq - cAq^N dt = 0. \quad (6)$$

The first relation is satisfied for curves passing through points 1 and 3, while the second is satisfied for curves passing through points 2 and 3 (see Fig. 1a). Using finite differences to approximate values of the differentials in Eqs. (6) (such as $dP = P_3 - P_1$) for the first characteristic curve), we obtain an algebraic system relative to the pressure and flow rate at point 3:

$$\frac{f}{\rho}P_3 + cq_3 = -\frac{Af}{\rho}q_1^N dz + \frac{f}{\rho}P_1 + cq_1;$$
$$P_3 - \frac{\rho c}{f}q_3 = Aq_2^N dz + P_2 - \frac{\rho c}{f}q_2. \quad (7)$$

Thus, the method of characteristics being used to solve the problem is based on the fact that we can determine the pressure and flow rate at the time $t + dt(P_3, q_3)$ if we know the distribution of pressure and flow rate along the entire channel at the moment t (the values P_1, q_1, P_2, q_2). One of the characteristic curves and the corresponding boundary condition (points 1' and 3' in Fig. 1a) are used to determine the running values of P_3 and q_3 in the upper sections of the channel. In the sections of the channel corresponding to the boundaries of the liquid and the gas-liquid packet and in the section where the liquid from the central pipe enters the annular pipe (z = 0), we match the solutions, i.e., different values of ρ, C, A, f, and h_j corresponding to the locus of the characteristic curves (such as for points 1"' and 2'" in Fig. 1a) are inserted into system (7) in the course of its solution).

After we determine the pressure and flow rate at the moment of time t + T, we proceed from the solution of system (7) for all points of the grid (j) to the next time step. We continue to do so until we have covered the entire time interval of interest to us.

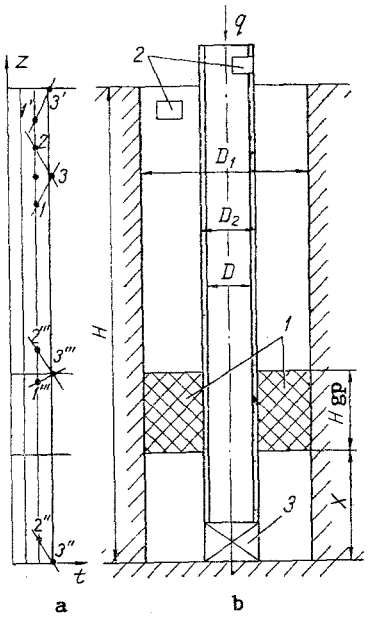

Fig. 1. Location of characteristic curves in the plane (z, t) (a) and general view of the channel, including the gasified packet (1), pressure gages (2), and pulse generator (3) (b).

As an example, we will examine the solution of the problem for the case when partial closure of the channel occurs at the bottom at z = 0. This leads to the formation of a pressure pulse that obeys Eq. (3). Meanwhile, we let $\Delta P_p^0 \approx 6 \cdot 10^5$ Pa; $\tau_{p2} = 1$ sec; $\tau_{p1} = 0.5$ sec; $k_1 = 0.5$; $k_2 = 1$. The compression wave formed in the central pipe ascends in the channel and after being attenuated somewhat by viscous friction is detected over a period of time $\Delta t \approx L/c$ by pressure gage 2 (see Fig. 1b). The rarefaction wave formed below the annular channel travels to the mouth and in the process also undergoes attenuation due to viscous friction. Meanwhile, the pressure gage 2, positioned several meters from the mouth of the annular pipe, records the wave with a certain lag due to its slowing by the amount Δt as a result of its passage along the gasified packet ($\Delta t \approx H_{gp}/c_\ell$). Solving this problem for different channel geometries (L, D, D_1, D_2), liquid densities and rheologies (ρ, K, N), gas-packet dimensions (H_{gp}), positions (X), gas contents (α), and types of gas (c_g, ρ_g), we can optimize the following parameters: the amplitude (ΔP_p^0), duration (τ_{p1}, τ_{p2}), and shape (k_1, k_2) of the pulse which should be detected by the gages located at the mouth of the channel. Here, by analyzing such solutions, we can better understand the physics of the processes connected with the propagation, attenuation, and reflection (at boundaries) of compression waves in such a complex channel. By setting the sensitivity and frequency characteristics of the sensors, we can also use the given mathematical model to determine their optimum location, the smallest (with respect to length and gas content) detectable (over Δt) gasified packets, and the accuracy of the method in relation to the parameters of the pulse and the model. It should be noted that the reflection from boundaries for plane harmonic waves depends on the ratio of the wave resistances ($\rho_i c_i$), since the reflection coefficient is equal to [6]:

$$K_{\text{ref}} = \frac{(\rho c)_1 - (\rho c)_2}{(\rho c)_1 + (\rho c)_2}. \tag{8}$$

Determining the values of $(\rho c)_i$, we can use Eqs. (2) to evaluate the reflection coefficient. For realistic values of the parameters of the model being examined, this coefficient ranges from 0.5 to 0.95.

Let us examine some of the results calculated for a specific model with the following parameters: L = 1500 m; D_1 = 0.204 m; D_2 = 0.114 m; D = 0.094 m; p_ℓ = 1100 kg/m^3; K = 0.287; N = 0.72; ρ_{g0} = 1.28 kg/m^3; α = 0.1; X = 500 m; H_{gp} = 150 m; c_ℓ = 1350 m/sec; c_g = 350 m/sec. The parameters of the pressure pulse excited at the bottom at z = 0 were described above.

Figure 2 shows pressure distributions obtained from the solution of the problem. It is evident from Fig. 2a that the two pressure pulses created by a temporary local resistance

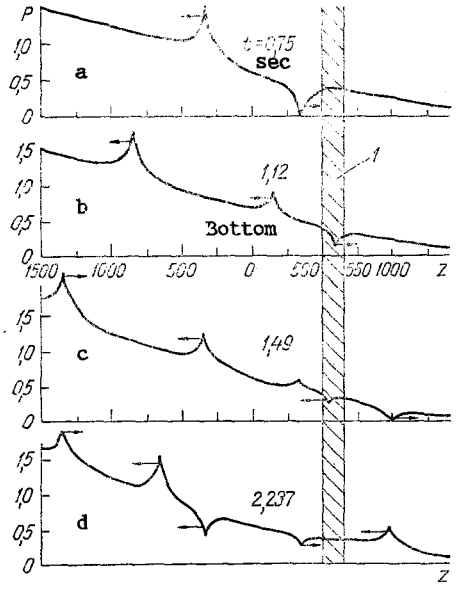

Fig. 2. Pressure distribution along the channel at different moments of time; 1) gasified packet. P, MPa; z, m.

at the bottom of the pipe (z = 0) travel about 350 m from the bottom by the moment t = 0.75 sec. However, since the fluid flow is directed downward in the central pipe, a compression wave develops in this pipe and a rarefaction wave develops in the annular pipe. It is evident from Fig. 2 – which shows the pressure distribution in the channel at t = 1.12 sec – that the rarefaction wave is partially reflected from the lower boundary of the gas–liquid packet as it travels through it. The reflected wave (2) is a compression wave because the reflection coefficient calculated for this boundary from (8) is negative. We also note that the distance travelled by wave (3) in the gas-liquid packet (ℓ_1) is shorter than the distance travelled by the reflected wave (ℓ_2). Meanwhile, $\ell_1/\ell_2 \approx c/c_g$ (c, determined from Eq. (2), is equal to about 395 m/sec). Compression wave (1) formed initially in the activation of the channel, continues to move toward the mouth of the central pipe at the velocity c_ℓ. The pressure maximum is formed about 0.5 sec after the beginning of operation (activation) of the channel. Thus, as follows from Fig. 2b, this pulse is then located the distance (1.12-0.05) × 1350 ≈ 840 m from the bottom.

In Fig. 2c (t = 1.49 sec), the total number of pulses formed inside the channel increases. The compression waves in the central part of the pipe move toward the mouth and correspond to the pulses connected with activation of the channel and reflection from the lower boundary of the gas–liquid packet.

The third pulse (Fig. 2c) is a compression wave formed by partial reflection, from the well bottom, of the pulse created by reflection from the lower boundary of the packet. Thus, the second and third pulses are located different distances from the bottom and move in opposite directions. The fourth and fifth pulses, being rarefaction waves, are formed with the passage and reflection of the initial pulse in the annular pipe through the upper boundary of the gas–liquid packet. Meanwhile, since the fourth pulse appears as a result of reflection from this boundary with a positive reflection coefficient, it too (as the transmitted pulse) is a rarefaction wave. All of the pressure pulses discussed above coincide in terms of time and velocity. Thus, the first, second, and third pulses are displaced in the liquid (relative to the pressure distribution at the preceding moment of time $\Delta t \approx 0.37$ sec) the distance $\ell = 0.37 \cdot 1350 \approx 500$ m. The third pulse travels about 150 m toward the bottom. Then, after reflection, it travels about 350 m in the opposite direction. The fourth pulse travels the distance $\ell = 0.37 \cdot 395 \approx 140$ m in the gasified packet during the same period of time. First this pulse travels in the direction of the boundary. After reflection, it then moves away from the boundary. The fifth pressure pulse travels about 50 m in the packet and 400 m in the annular pipe during the above-indicated time, i.e., the total time of its motion is equal to $\Delta t = 50/395 + 400/1350 \approx 0.4$ sec. Figure 2d shows the pressure distribution along the channel at the time t = 2.237 sec. It is found to be even more complex in character than the previous distribution, due to multiple reflections on the boundaries and the bottom. Here, we will note only the main features. The first and second

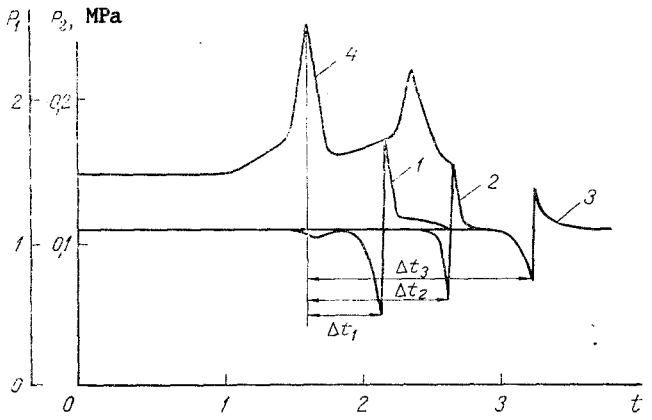

Fig. 3. Pressure change at the mouth of the central pipe (P_1) and the annular channel (P_2) over time for different lengths of gasified packet (H_{gp}) (X = 500 m; α = 0.5): 1) P_2 at H_{gp} = 150 m; 2) 300; 3) 450; 4) P_1 at any H_{gp}.

pulses, being compression waves traveling through the central pipe, are connected with reflection from the lower boundary of the packet and the mouth of this pipe (2). It should be mentioned that they move in opposite directions and that the first pulse is smaller in amplitude than the second. The third pulse is a rarefaction wave which develops due to reflection from the upper boundary of the packet. Its partial reflection when it passes through the bottom (z = 0) accounts for the fact that the fourth and third pulses are located the same distance from the bottom and move in opposite directions. The fifth pulse is a compression wave which arises from the reflection of the rarefaction wave from the free surface at the mouth of the annular pipe.

The pattern of pressure distribution along the channel subsequently has a tendency both toward the appearance of an even greater number of pulses (due to reradiation at boundaries) and toward their gradual decay. The rate of pulse attenuation here depends on the rheology of the liquid, and complete attenuation occurs 10-20 sec after the beginning of the process for actual viscous liquids.

As was shown by calculations performed with the given model, a twofold change in the viscosity of the liquid (for K = 0.574) is accompanied by a decrease in the amplitude of the pressure pulse arriving at the mouth of the channel $\Delta P_1(t)$ from 1.05 to 0.6 MPa.

It should be noted that the pulses connected with the transmission of the compression waves which are generated upon activation of the channel in the central and annular pipes make it possible to detect the presence of a gasified packet from the magnitude of the lag time Δt. Figure 3 shows results of calculations performed with the given model for different packet lengths with a gas content α = 0.5. These results illustrate well the essence of the method in [4] and agre with the experimental curves presented there.

We can draw the following conclusions from numerous computer calculations performed with the given model for different parameters characterizing the propagation of dynamic disturbances in a channel.

1. A pressure pulse of several atmospheres lasting from tenths of a second to several seconds travels from 10,000 to 20,000 m in a long channel filled with a viscous non-Newtonian fluid before it undergoes complete attenuation. The time of attenuation depends on the viscosity of the liquid and the cross section of the channel.

2. A compression wave is more easily detected from the end of the channel where pressure is maintained to inject the liquid than it is near the free surface of the liquid at the mouth of the annular pipe (a more sensitive transducer is required in the latter case). If the latter approach is used, it is necessary to place the transducer some distance from the surface.

3. The presence of a gas-liquid packet in the channel lowers the amplitude of the signal that reaches the mouth. This occurs because the attenuation caused by viscous friction is augmented by reflection of the signal at two interfaces. The attenuating effect of the reflections increases with an increase in gas content due to an increase in the reflection coefficient.

4. With the passage of a pressure pulse through an interface between two media in the case when the wave resistance (ρc) of the second medium is lower (lower boundary of the packet, free surface), the reflected compression wave changes sign but the velocity remains the same. In the case when the wave resistance of the second medium is greater (upper boundary of the packet, well bottom, mouth of the central tube), the reflected compression wave retains its sign and the velocity changes to the opposite value.

5. The transmitted pressure pulse always retains the sign of the transmitted wave. Meanwhile, the amplitudes of the pressure pulses and the velocities of the incident, transmitted, and reflected (from the interface) waves are such as to satisfy the condition of equality of the total pressures and the normal components of velocity at the boundary.

NOTATION

$P(z, t)$, pressure in the channel; $q(z, t)$, volumetric flow rate of liquid; ρ, density of liquid; c, velocity of dynamic disturbances in the fluid; τ, shear stress; $\delta = f/\ell$, corrected hydraulic radius of pipe; f, cross section of channel; ℓ, perimeter of channel; α, gas content; ρ_g, ρ_ℓ, density of gas and liquid; c_g, c_ℓ, speed of sound in the gas and liquid; ρ_{g0}, density of gas under atmospheric conditions (at $P = P_{atm}$); K, N, constants in the exponential rheological model of the liquid; K_{ref}, reflection coefficient; L, length of channel; X, distance from the bottom to the lower boundary of the paket; D, D_2, inside and outside diameters of pipe; D_1, inside diameter of external pipe of the annular channel; H_{gp}, height of the gasified packet.

LITERATURE CITED

1. G. D. Rozenberg and I. V. Magdalinskaya, Dokl. Akad. Nauk SSSR, 255, No. 4, 625-627 (1980).
2. I. A. Charnyi, Nonsteady Motion of an Actual Liquid in Pipes [in Russian], Moscow (1975).
3. S. D. Tseitlin, Inzh. Fiz. Zh., 40, No. 4, 664-672 (1981).
4. A. M. Yasashin and R. V. Avetov, Neft. Khoz., No. 11, 24-27 (1980).
5. G. Wallace, One-Dimensional Two-Phase Flows [Russian translation], Moscow (1972).
6. L. M. Brekhovskikh and V. V. Goncharov, Introduction to Continuum Mechanics [in Russian], Moscow (1982).

NUMERICAL INVESTIGATION OF NONEQUILIBRIUM TWO-PHASE FLOWS IN AXISYMMETRIC LAVAL NOZZLES

P. M. Kolesnikov and V. V. Leskovets

UDC 533.6.011.3

A computation algorithm is elucidated and results are presented of the numerical solution of two-phase flow equations. A comparison is made with the experimental and computed data of other authors.

Flows of two-phase mixtures consisting of a gas and particles or drops suspended therein are extensively widespread in both nature and in technical applications. A set of typical examples of such two-phase flows can be presented. Certain of the natural phenomena are the motion of raindrops or snow in clouds and mist, dust and sand storms, scattering of particles of different origin in the atmosphere, etc. A broad circle of applied problems is associated with the flow and application of aerosols of different kinds, intensification of the heat and mass transfer processes in chemical production, natural gas transport, thermal and mechanical treatment of friable materials, etc.

Aviation and cosmonautics also inevitably encounter the solution of theoretical problems and the performance of extensive testing investigations in this area. Great value is attrib-

A. B. Lykov Institute of Mass and Heat Transfer, Academy of Sciences of the Belorussian SSR, Minsk.

Translated from Inzhenerno-Fizicheskii Zhurnal, Vol. 8, No. 1, pp. 27-35, January, 1990. Original article submitted September 26, 1988.

0022-0841/90/5801-0020$12.50